NUCLEAR STRUCTURE AND ISOBAR COLLISIONS

HAOJIE XU (徐浩洁)

HUZHOU UNIVERSITY(湖州师范学院)

IN COLLABORATION WITH:

LIE-WEN CHEN, HANLIN LI, ZIWEI LIN, CAIWAN SHEN, FUQIANG WANG,

XIAOBAO WANG, HANZHONG ZHANG, JIE ZHAO, YING ZHOU.

THE 6TH INTERNATIONAL CONFERENCE ON CHIRALITY, VORTICITY AND MAGNETIC FIELD IN HEAVY ION COLLISIONS

1-5 NOVEMBER 2021, STONY BROOK UNIVERSITY

Relativistic Heavy ion collisions

Woods-Saxon distributions

$$\rho(r) = \frac{\rho_0}{1 + \exp[(r - R)/a]}$$

$$R = R_0\,[1+\beta_2 Y_2^0(\theta)+\beta_4 Y_4^0(\theta)]$$

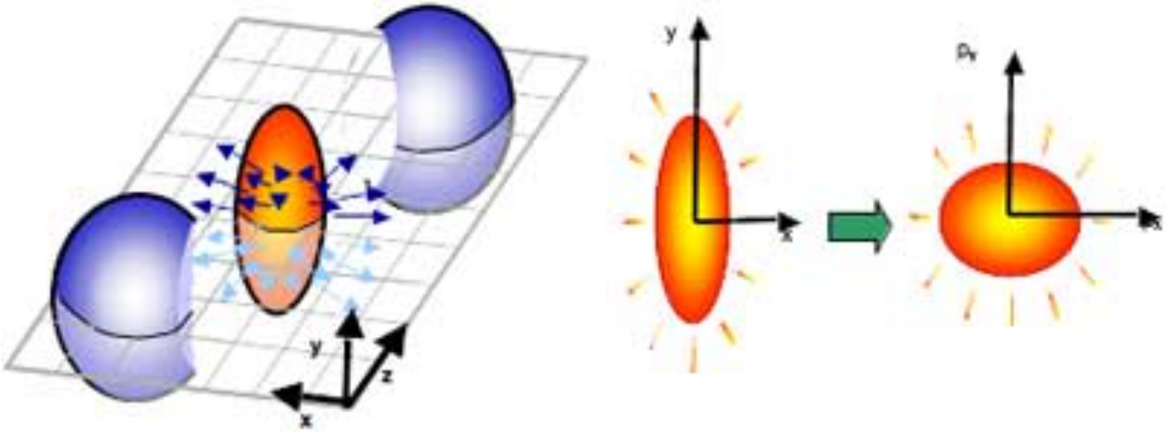

Anisotropic flow,
Flow fluctuations
HBT,
....

Initial geometry

Bulk properties of QGP medium: $\eta/s, \zeta/s, \ldots$

Final observables

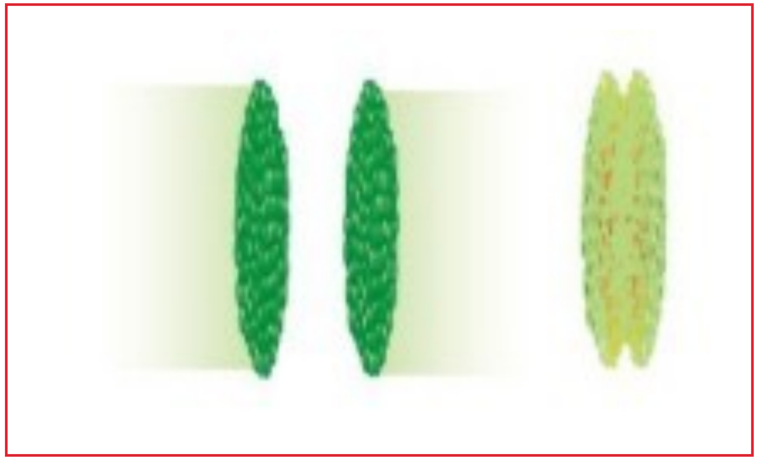

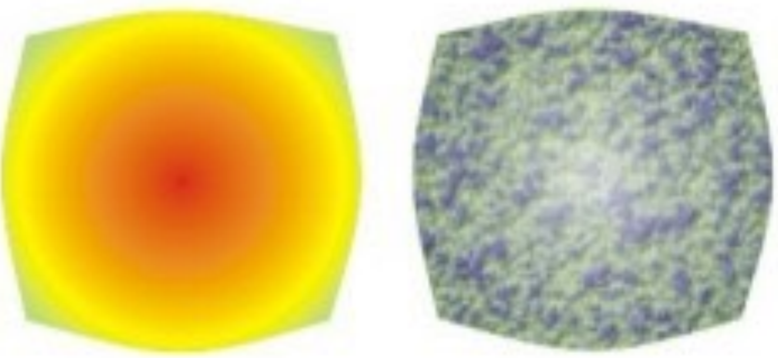

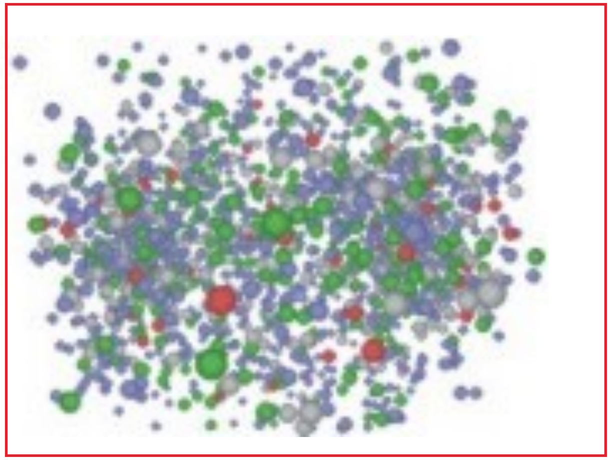

Relativistic isobaric collisions

The isobar collisions was proposed to measure the chiral magnetic effect. S. Voloshin, PRL105, 172301 (2010)

$\sqrt{s_{NN}} = 200$ GeV

$^{96}_{40}Zr + ^{96}_{40}Zr$ $^{96}_{44}Ru + ^{96}_{44}Ru$

	R	a	β_2
Zr	5.02	0.46	0.08/0.217
Ru	5.085	0.46	0.158/0.053

WS parameters extracted from charge density distributions

W. Deng, X. Huang, et.al., PRC94,041901(2016)

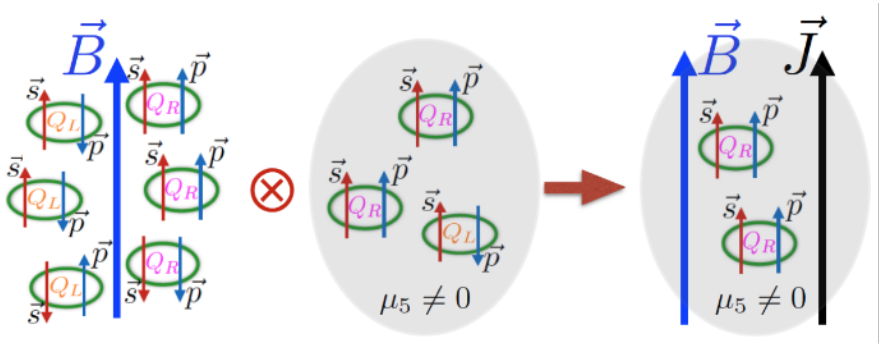

Chiral magnetic effect (CME)

$$\mathbf{J}_{\mathbf{cme}} = \sigma_5 \mathbf{B} = \left(\frac{(Qe)^2}{2\pi^2}\mu_5\right)\mathbf{B},$$

D. Kharzeev,et.al., PPNP88, 1(2016)

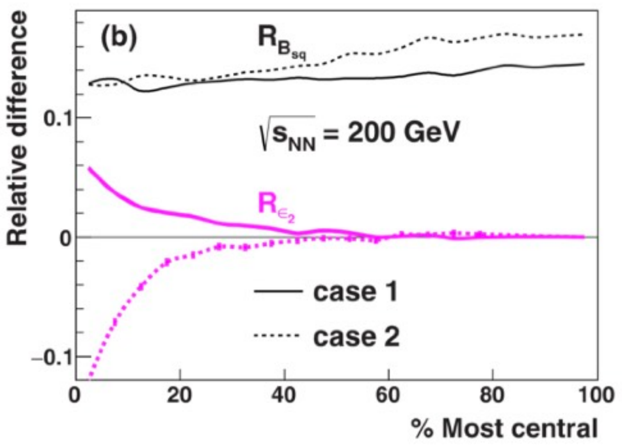

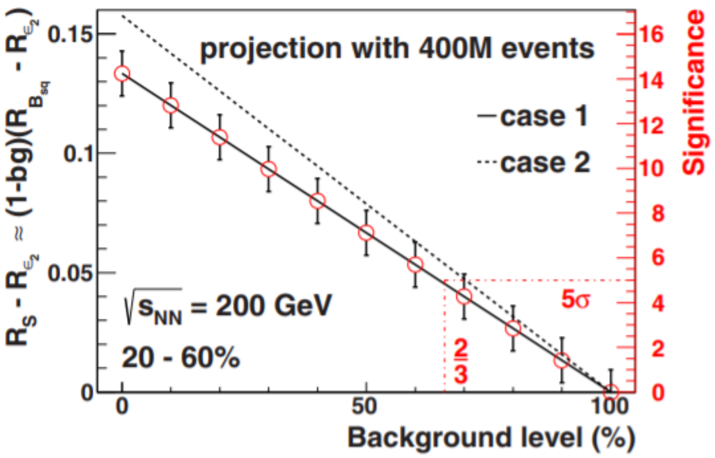

- Same eccentricities => same flow background
- Different magnetic field => different CME signals

Neutron skin and symmetry energy

Charge density $\neq$ nuclear density.

Nuclear density distribution:

- Proton distribution — Can be accurately measured in experiment.
- Neutron distribution — Poorly known

Neutron skin: RMS radii differences between neutron distribution and proton distribution

$$\Delta r_{np} \equiv \sqrt{\langle r_n^2 \rangle} - \sqrt{\langle r_p^2 \rangle}$$

Neutron skin depends on symmetry energy:

$$E(\rho,\delta) = E_0(\rho) + E_{\rm sym}(\rho)\delta^2 + O(\delta^4)$$

$$\rho = \rho_n + \rho_p;\ \delta = \frac{\rho_n - \rho_p}{\rho}$$

$$L(\rho_c) = 3\rho_c \left[\frac{dE_{\rm sym}(\rho)}{d\rho}\right]_{\rho=\rho_c};\ \rho_c \simeq 0.11{\rm fm}^{-3}$$

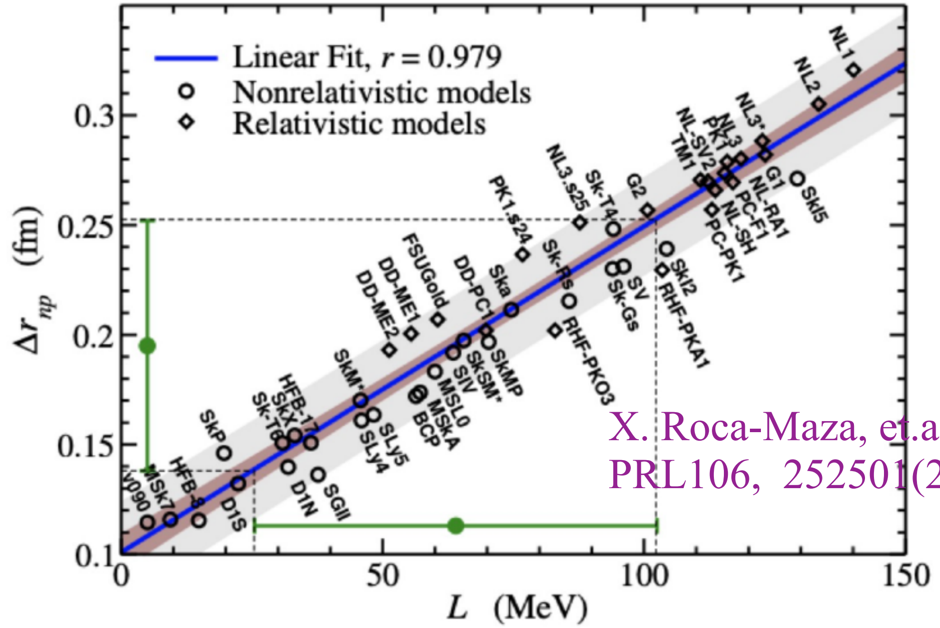

X. Roca-Maza, et.al., PRL106, 252501(2011)

The symmetry energy is crucial to our understanding of the masses and drip lines of neutron-rich nuclei and the equation of state (EOS) of nuclear and neutron star matter.

Charge densities and nuclear density in isobar collisions

- **Charge density ≠ nuclear density.**

HJX, et.al., PRL121, 022301 (2018)
H. Li, HJX, et.al., PRC98, 054907(2018)

Normally we assume neutron density profile = proton's. It's mostly ok, but for the CME search where the signal is small and we rely on large cancellation of backgrounds between two systems, we should take the difference between neutron and proton densities into consideration.

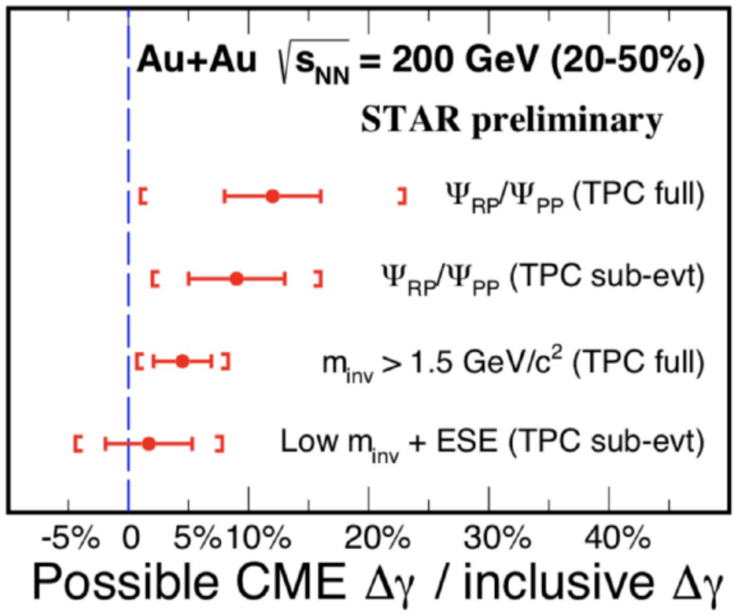

STAR Collaboration, NPA982, 535(2019)

Background dominated
--- The CME signal, if exist, is very small

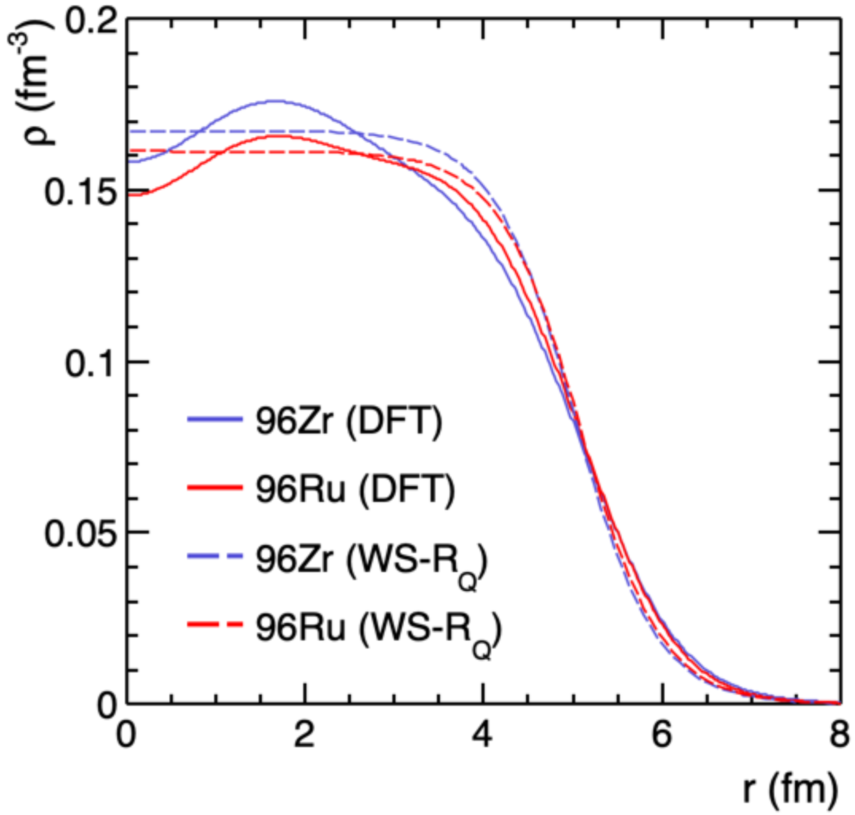

- Instead of the WS densities with parameters extracted from the measured charge densities, we use the proton and neutron densities obtained from the energy density functional theory (DFT) with Skyrme parameter set SLy4.

Multiplicity distribution difference between isobars

Predictions with charge densities

W. Deng, et.al., PRC94,041901(2016)

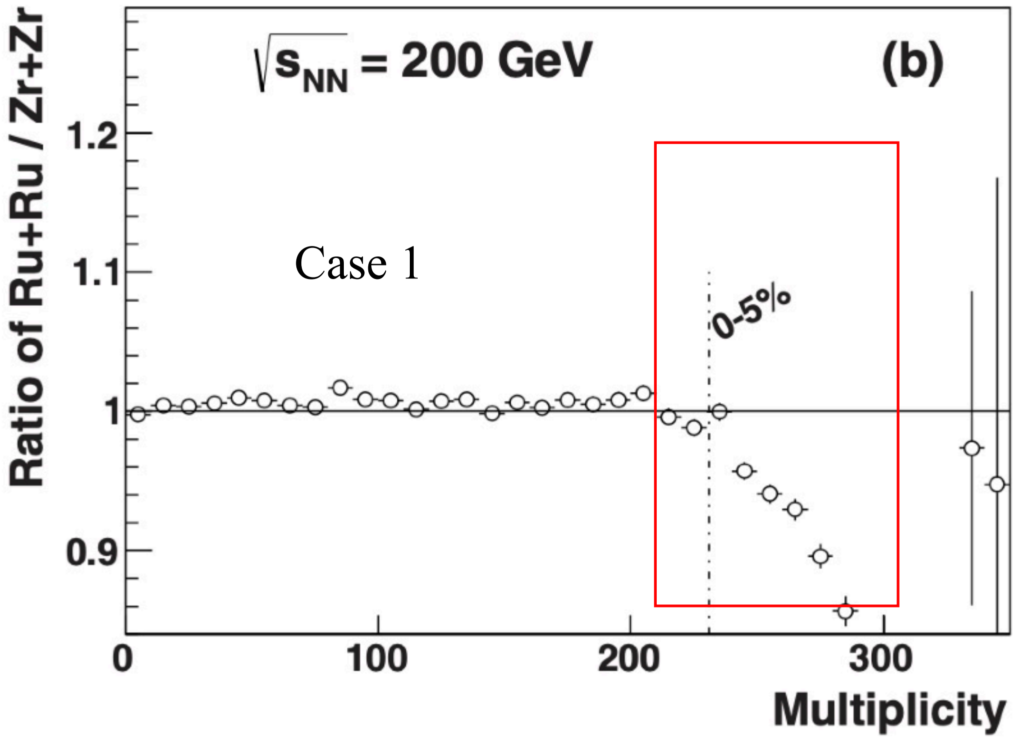

Predictions with DFT densities

H. Li, HJX, et.al., PRC98, 054907(2018)

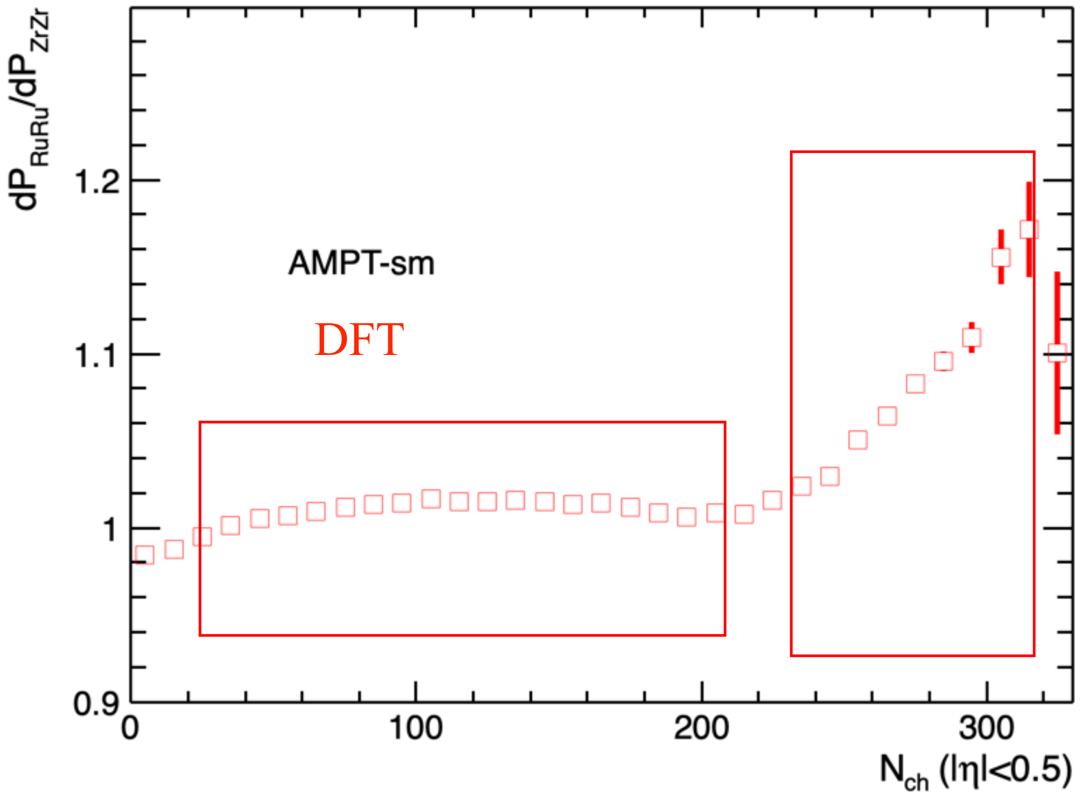

Opposite predictions from WS charge densities and DFT densities (neutron skins)

DFT predictions of multiplicity ratio are verified by STAR data

H. Li, HJX, et.al., PRC98, 054907(2018)

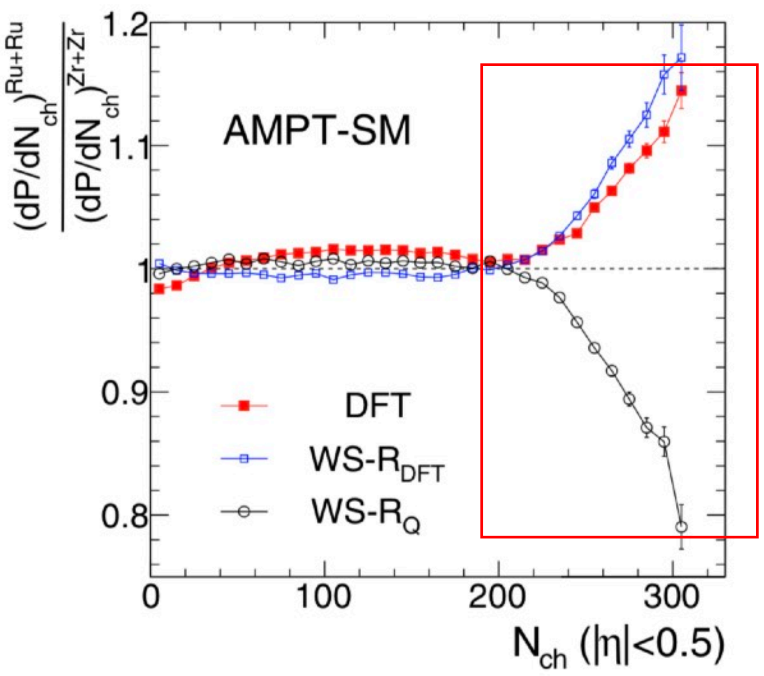

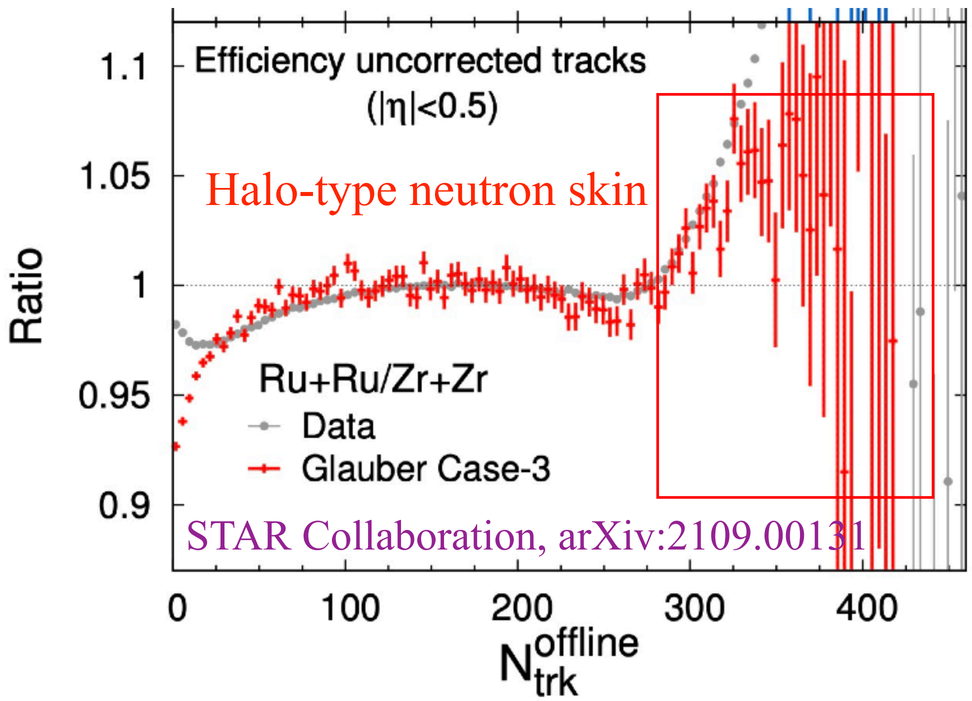

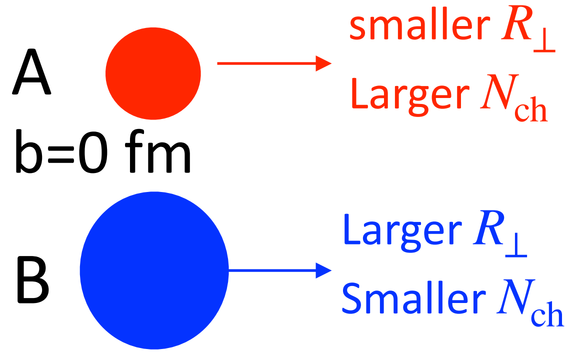

$$\left(\sqrt{\langle r_{ch}^2\rangle}\right)_{Ru} > \left(\sqrt{\langle r_{ch}^2\rangle}\right)_{Zr}$$

$$\left(\sqrt{\langle r_{DFT}^2\rangle}\right)_{Ru} < \left(\sqrt{\langle r_{DFT}^2\rangle}\right)_{Zr}$$

- The previous WS parameters extracted from charge density distributions (Ru larger than Zr) give opposite behavior to data
- The DFT densities give the correct behavior of the data ratio, because Ru is smaller than Zr from DFT calculation.
- The WS densities with the R parameter adjusted to the effective DFT radii (skin-type) give similar prediction on the tail but miss the medium multiplicity range.

v_2 difference between isobars

Predictions from charge densities with deformation

W. Deng, et.al., PRC94,041901(2016)

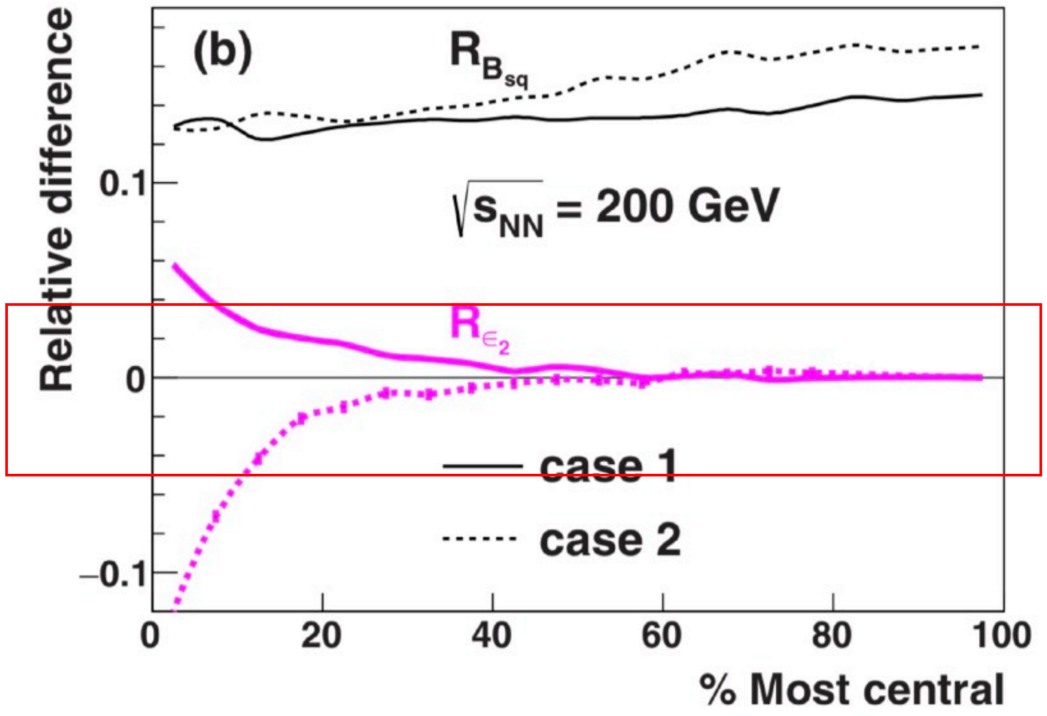

Predictions from DFT densities without deformation

HJX, et.al., PRL121, 022301 (2018)

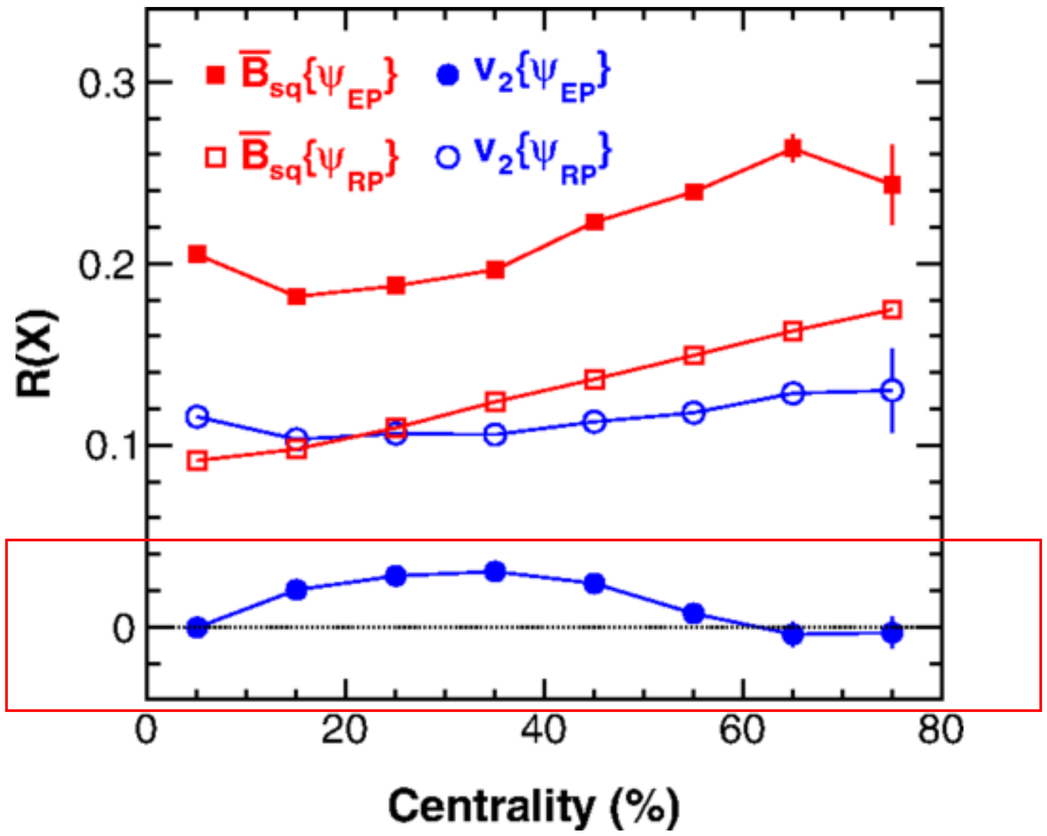

Compare to the predictions from charge densities, the calculations with DFT densities indicate that the Zr+Zr collisions and Ru+Ru collisions **have sizable differences in v_2 in 20-50% centrality range**.

DFT predictions of v_2 ratios are "verified" by STAR data

HJX, et.al., PLB819, 136453 (2021)

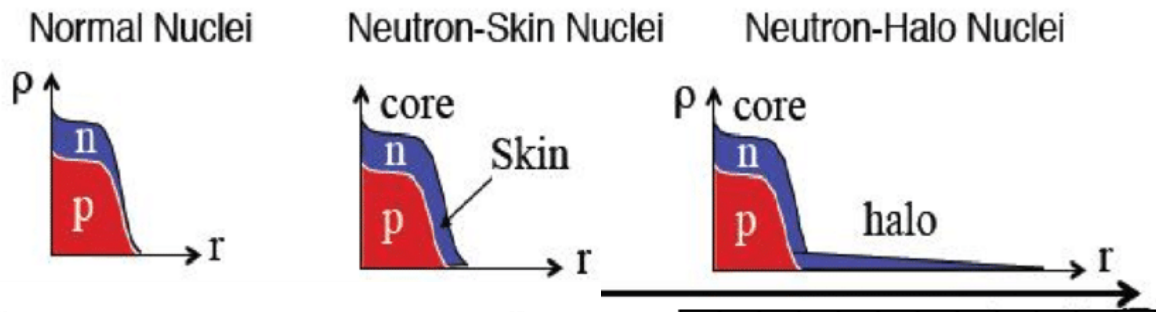

- Neutron-skin nuclei and neutron-halo nuclei for Zr

	^{96}Ru		^{96}Zr	
	R	*a*	*R*	*a*
p	5.085	0.523	5.021	0.523
skin-type n	5.085	0.523	5.194	0.523
halo-type n	5.085	0.523	5.021	0.592

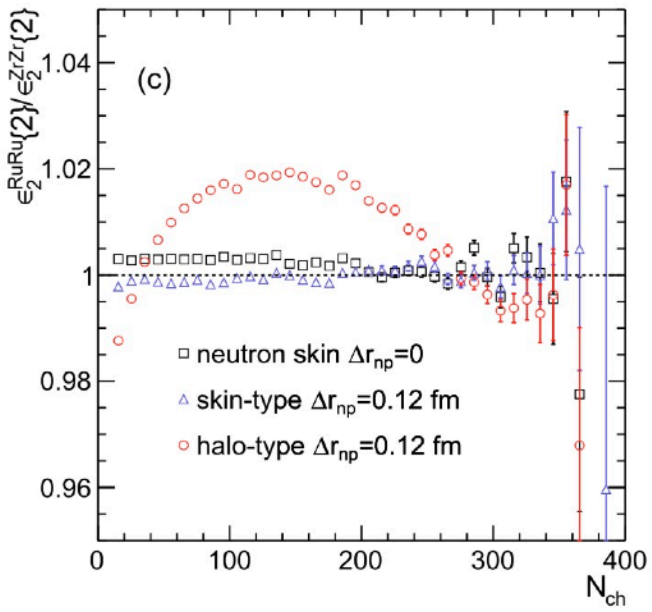

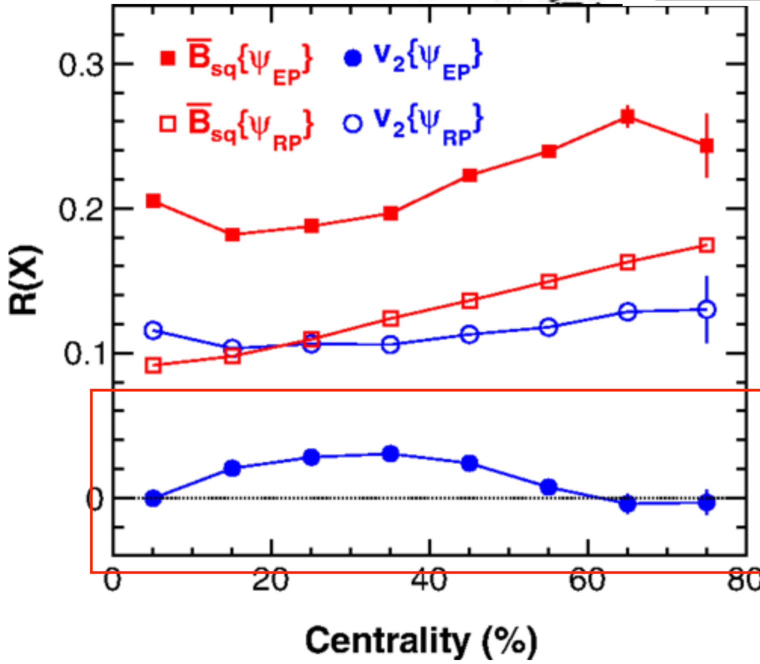

STAR Collaboration, arXiv:2109.00131

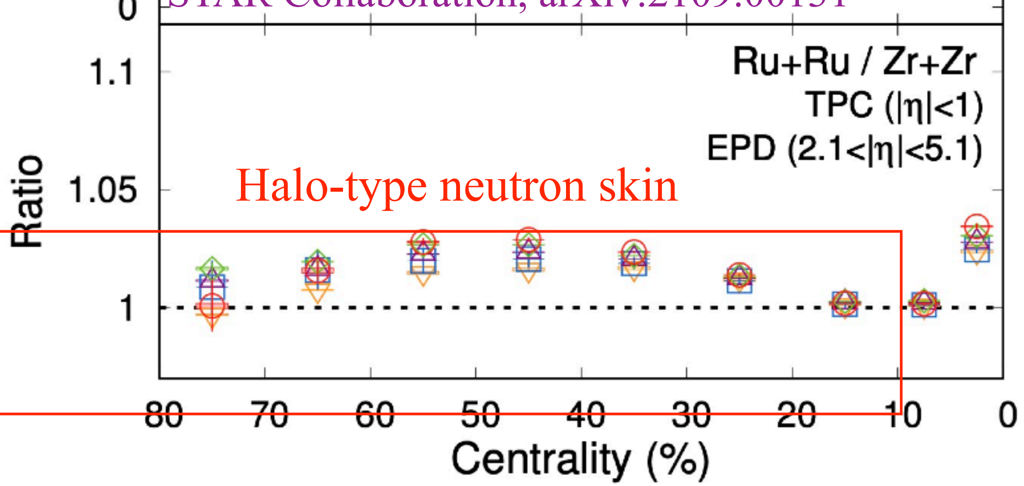

The shapes of the Ru+Ru/Zr+Zr ratios of the eccentricity in mid-central collisions can further distinguish between skin-type and halo-type neutron densities.

A summary of what we've learned so far

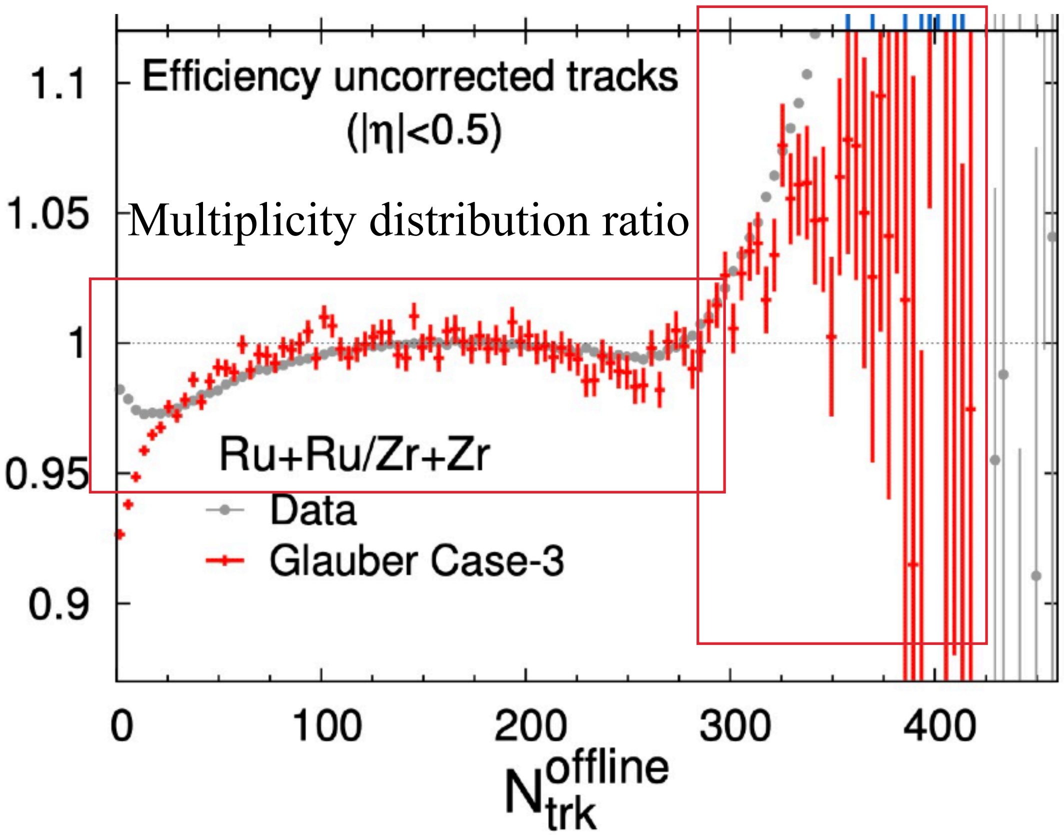

STAR Collaboration, arXiv:2109.00131

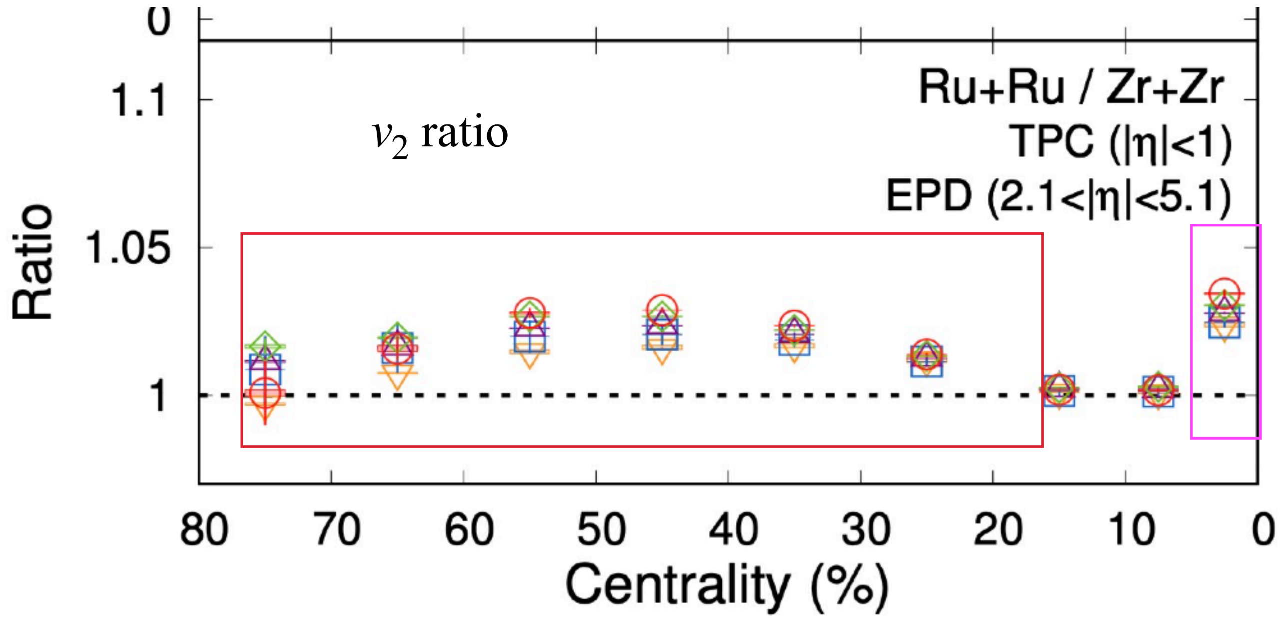

- STAR data indicate a thick neutron skin for the Zr nuclei, consistent with DFT predictions
- STAR data indicate a halo-type neutron skin, also consistent with DFT predictions
- Sizable v_2 and v_3 ratios in most central collisions may indicate shape difference in isobars. (Jiangyong's talk)

Isobar structures are important for the CME search

STAR Collaboration, arXiv:2109.00131

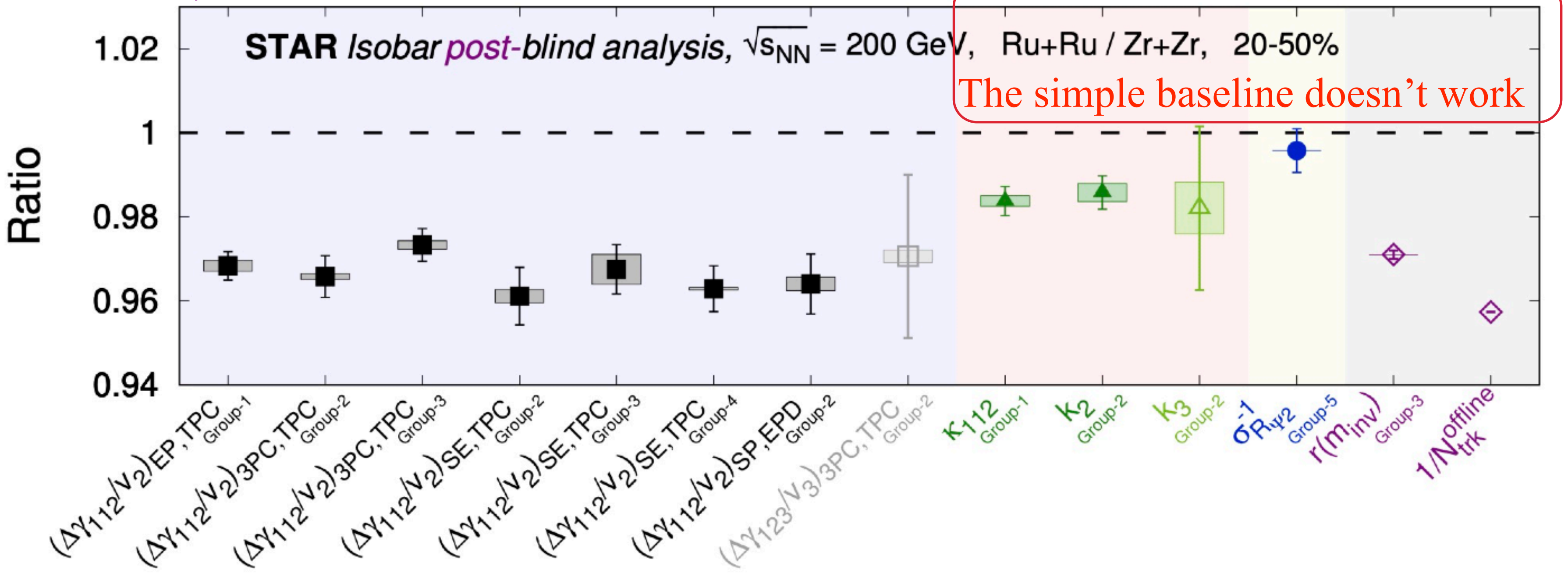

$$\Delta\gamma_{\rm bkg} = \langle \cos(\varphi_\alpha + \varphi_\beta - 2\Psi_{RP}) \rangle = \frac{N_{\rm cluster}}{N_\alpha N_\beta} \times \langle \cos(\varphi_\alpha + \varphi_\beta - 2\Psi_{\rm cluster}) \rangle \times v_{2,{\rm cluster}}$$

Multiplicity differences

Flow differences

The multiplicity and v2 differences from isobar structure are crucial for the CME search in the isobar collisions at RHIC

We can do more …

Probing the neutron skin with relativistic isobaric collisions

- Multiplicity ratio
- $\langle p_T \rangle$ ratio
- Net-charge ratio in very peripheral collisions

Current status of neutron skin measurements

PREX-2 Collaboration, PRL126, 172502(2021); B. Reed, et.al., PRL126, 172503(2021)

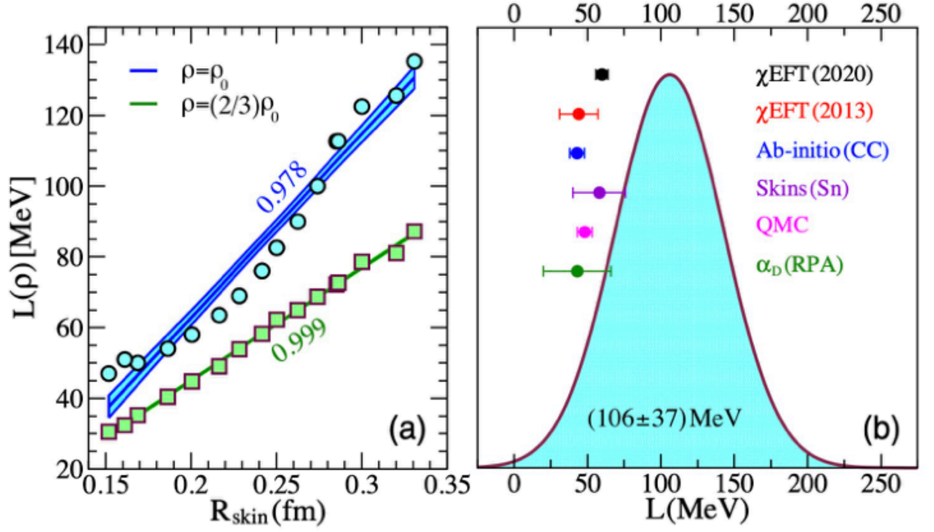

FIG. 1. Left: slope of the symmetry energy at nuclear saturation density ρ_0 (blue upper line) and at $(2/3)\rho_0$ (green lower line) as a function of $R^{208}_{\rm skin}$. The numbers next to the lines denote values for the correlation coefficients. Right: Gaussian probability distribution for the slope of the symmetry energy $L = L(\rho_0)$ inferred by combining the linear correlation in the left figure with the recently reported PREX-2 limit. The six error bars are constraints on L obtained by using different theoretical approaches [14,19–25].

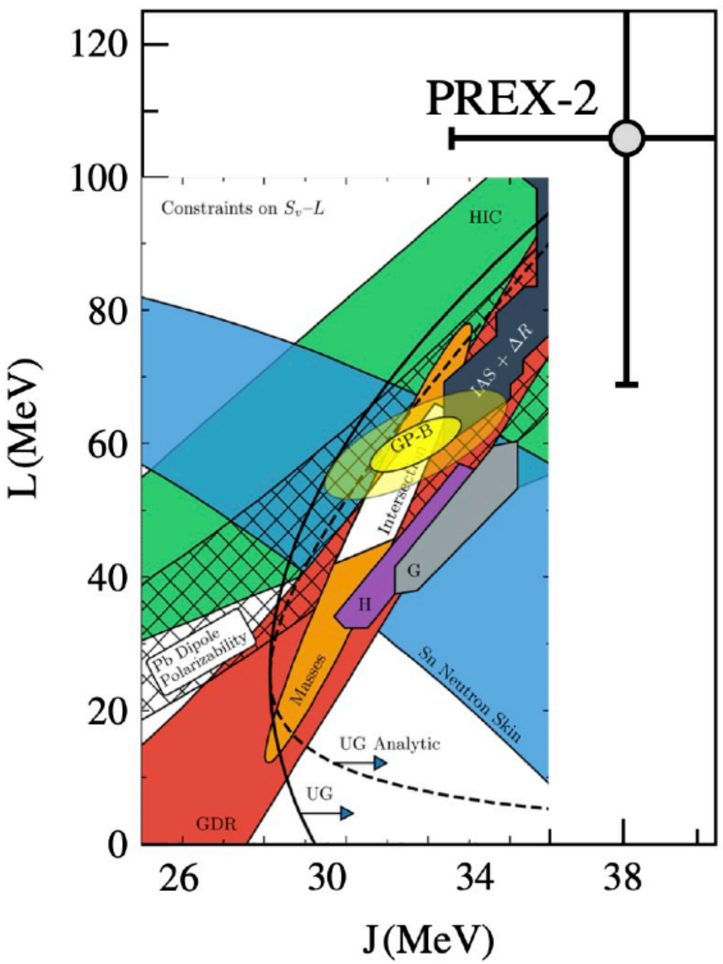

$$\Delta r_{\rm np}^{\rm Pb} = (0.284 \pm 0.071)\ \text{fm}$$

$$L(\rho_0) = (106 \pm 37)\ \text{MeV}$$

$$L(\rho_c) = (71.5 \pm 22.6)\ \text{MeV}$$

This PREX-2 result favors a large neutron skin thickness and symmetry energy slope parameter, at tension with existing experimental data and theoretical analyses.

Neutron skin and nuclear symmetry energy

H. Li, HJX, et.al., PRL125, 222301(2020)

SHF: Standard Skyrme-Hartree-Fock (SHF) model
eSHF: Extended SHF model

$$E(\rho,\delta) = E_0(\rho) + E_{\rm sym}(\rho)\delta^2 + O(\delta^4)$$

$$\rho = \rho_n + \rho_p;\ \ \delta = \frac{\rho_n - \rho_p}{\rho}$$

$$L(\rho_c) = 3\rho_c \left[\frac{dE_{\rm sym}(\rho)}{d\rho}\right]_{\rho=\rho_c};\ \ \rho_c \simeq 0.11 {\rm fm}^{-3}$$

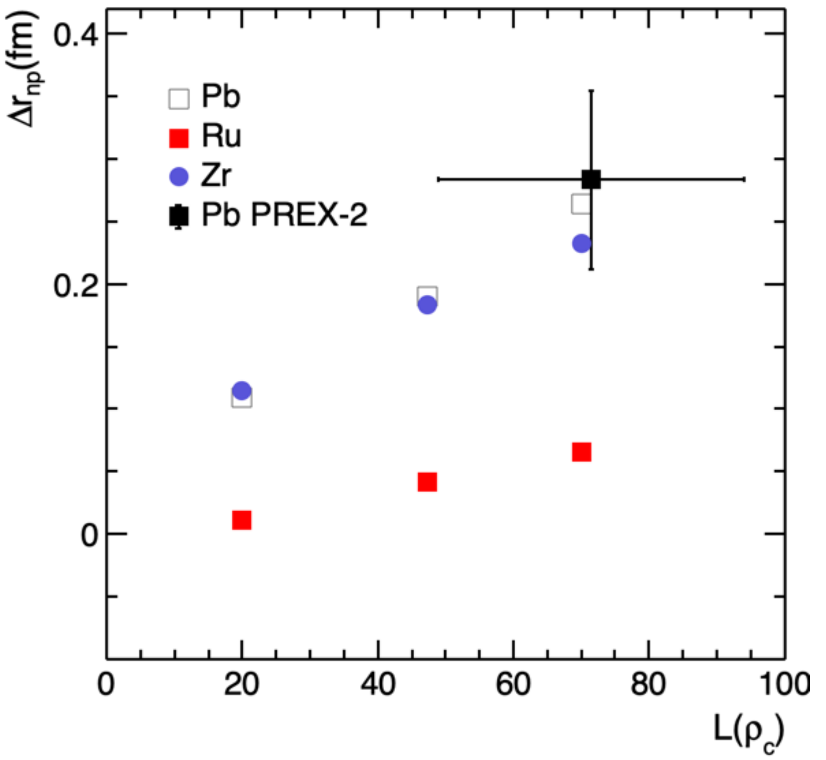

Lc20
Lc47
Lc70

Z. Zhang, PRC94, 064326(2016)

$$\begin{aligned} v_{i,j} &= t_0(1+x_0P_\sigma)\delta(\mathbf{r}) + \frac{1}{6}t_3(1+x_3P_\sigma)\rho^\alpha(\mathbf{R})\delta(\mathbf{r}) \\ &+ \frac{1}{2}t_1(1+x_1P_\sigma)[K'^2\delta(\mathbf{r}) + \delta(\mathbf{r})K^2] \\ &+ t_2(1+x_2P_\sigma)\mathbf{K}'\cdot\delta(\mathbf{r})\mathbf{K} \\ &+ \frac{1}{2}t_4(1+x_4P_\sigma)[K'^2\delta(\mathbf{r})\rho(\mathbf{R}) + \rho(\mathbf{R})\delta(\mathbf{r})K^2] \\ &+ t_5(1+x_5P_\sigma)\mathbf{K}'\cdot\rho(\mathbf{R})\delta(\mathbf{r})\mathbf{K} \\ &+ iW_0(\boldsymbol{\sigma}_i+\boldsymbol{\sigma}_j)\cdot[\mathbf{K}'\times\delta(\mathbf{r})\mathbf{K}], \qquad (4) \end{aligned}$$

Extended

			^{96}Zr			^{96}Ru			^{208}Pb
	$L(\rho_c)$	$L(\rho_0)$	r_n	r_p	Δr_{np}	r_n	r_p	Δr_{np}	Δr_{np}
Lc20	20	13.1	4.386	4.27	0.115	4.327	4.316	0.011	0.109
Lc47	47.3	55.7	4.449	4.267	0.183	4.360	4.319	0.042	0.190
Lc70	70	90.0	4.494	4.262	0.232	4.385	4.32	0.066	0.264
SLy4	42.7	46.0	4.432	4.271	0.161	4.356	4.327	0.030	0.160

Method I: multiplicity distribution ratio

H. Li, HJX, et.al., PRL125, 222301(2020)

Lc47: DFT calculations using data from terrestrial nuclear experiments and astrophysical observations.
Y. Zhou, L. Chen, Z. Zhang, PRD99, 121301R(2021)

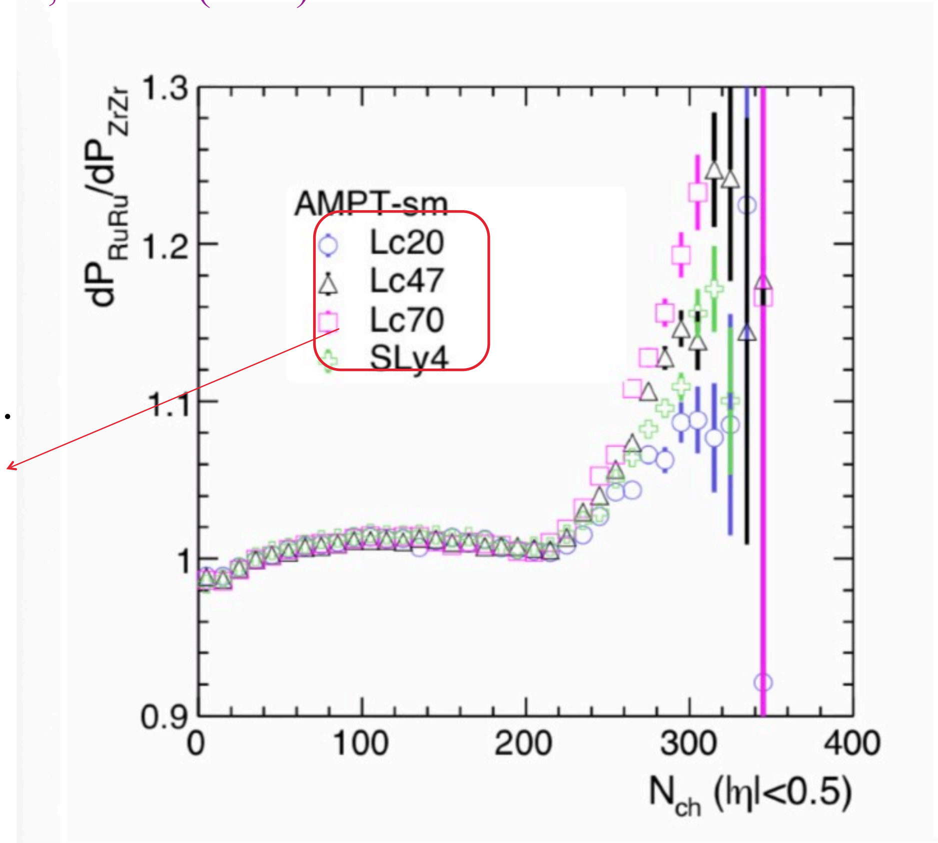

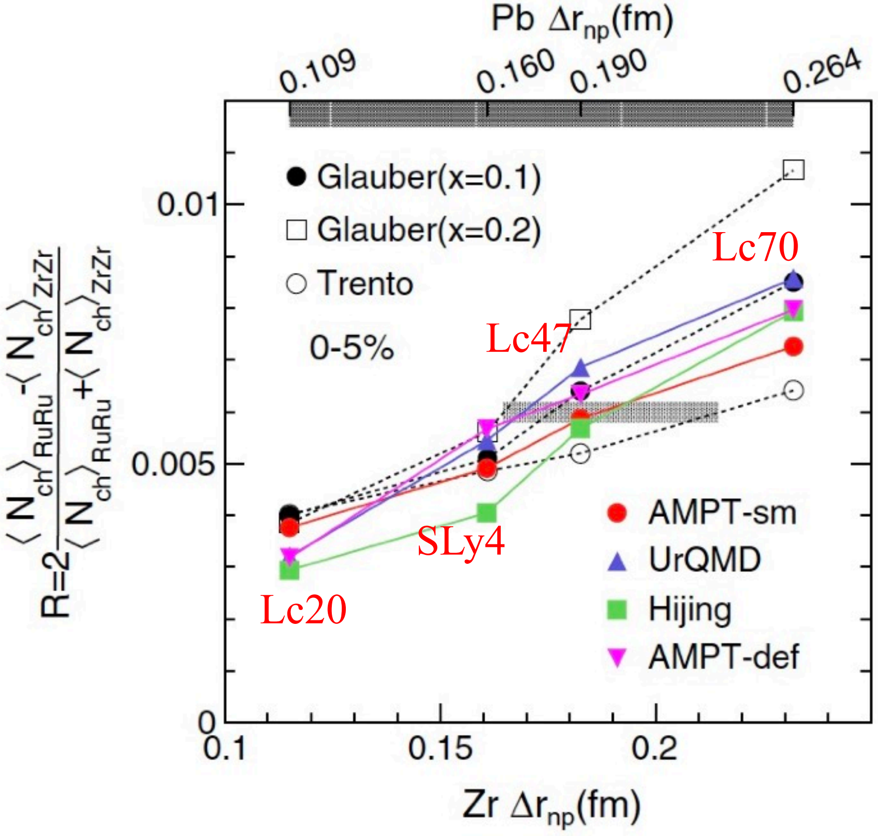

- The ratio of N_{ch} distributions highlight the differences
- To quantify the differences, we use the R observable of N_{ch} at top 5% centrality.
- R is a relative measure, **much of experimental effects cancel**

Method II: mean p_T ratio

HJX, et.al, in preparation

b=0 fm

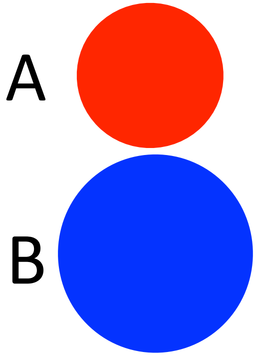

A → smaller $R_\perp$ → larger N_{ch} and $\langle p_T \rangle$

B → Larger $R_\perp$ → Smaller N_{ch} and $\langle p_T \rangle$

$R(\langle p_T \rangle) \propto 1/R(\langle \sqrt{r^2} \rangle)$

Lc47: DFT calculations using data from terrestrial nuclear experiments and astrophysical observations.
Y. Zhou, L. Chen, Z. Zhang, PRD99, 121301R(2021)

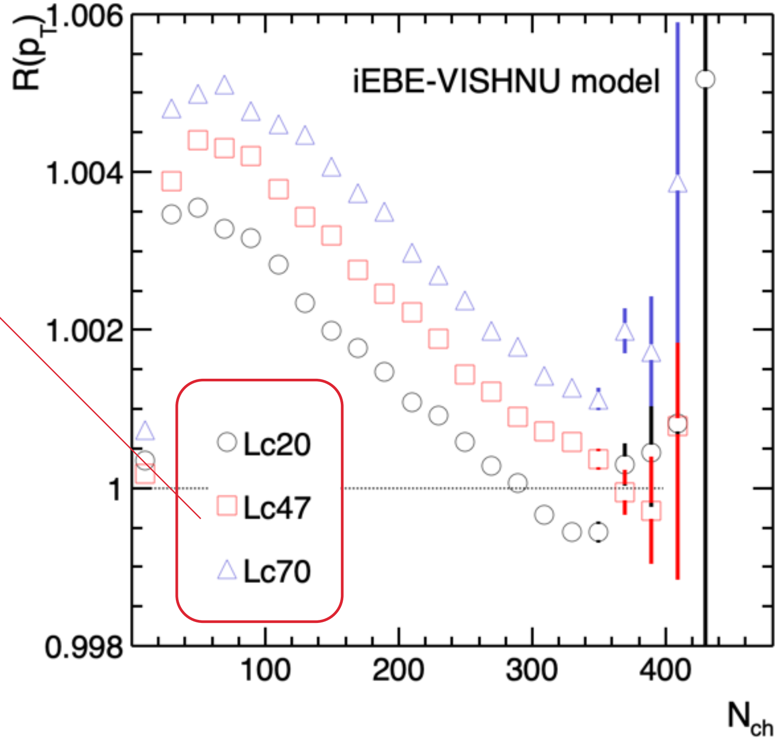

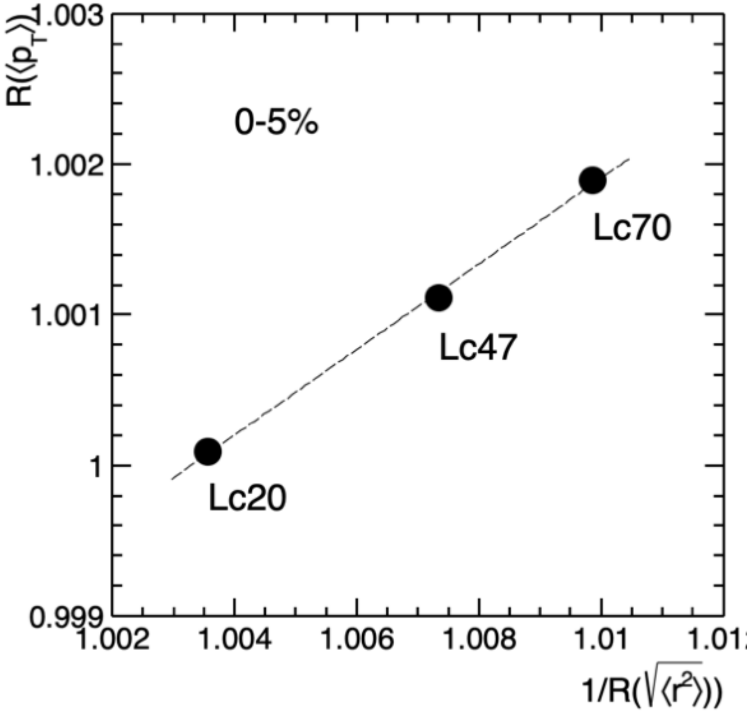

The $R(\langle p_T \rangle)$ is inversely proportional to nuclear size ratio in most central collisions.

Method III: net-charge ratio in very peripheral collisions

HJX, et.al., arXiv:2105.04052 (2021)

For the colliding nuclei with large neutron skin thickness

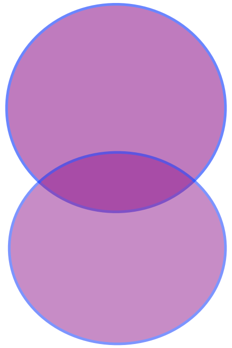

→ more n+n collisions at most peripheral collisions → Less participant charges, thus less final net-charges

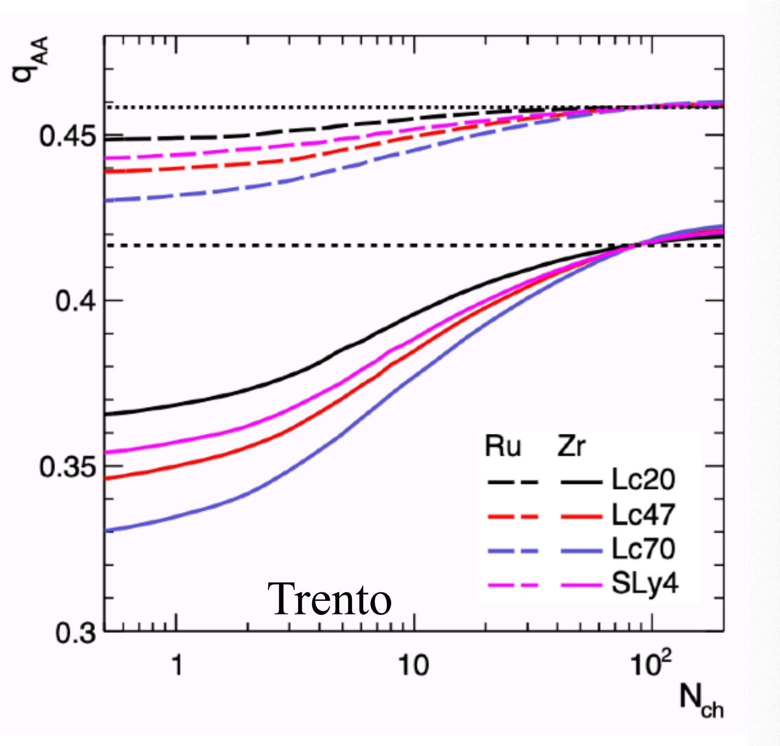

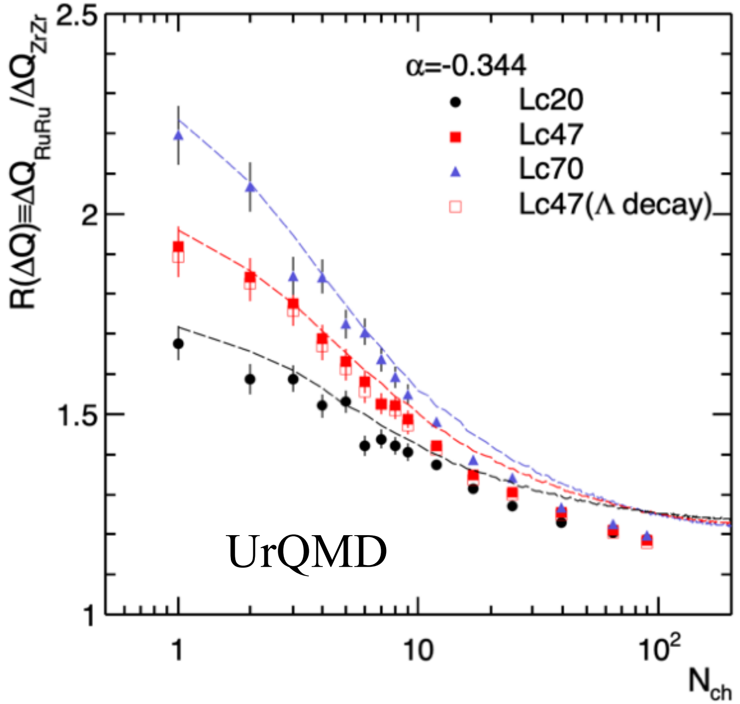

The curves are calculated by superimposition assumption

$$R(\Delta Q) = \frac{q_{RuRu} + \alpha/(1-\alpha)}{q_{ZrZr} + \alpha/(1-\alpha)}$$

where $q_{RuRu/ZrZr}$ are the fraction of protons among the participant nucleons, obtained by the Trento model.

α is the ΔQ ratio in nn to pp interaction:

Pytha: $\alpha = -0.352$

Hijing: $\alpha = -0.389$

UrQMD: $\alpha = -0.344$

SUMMARY

- The STAR isobar data indicate **thick halo-type neutron skin in Zr**, consistent with **DFT** calculations.
- The size and structure differences cause multiplicity and v2 differences, **crucial for the CME search**.
- Ultra-relativistic iosbar collisions can be used to **probe the neutron skin and symmetry energy**
  - Multiplicity distribution ratio; Mean p_T ratio; Net charge ratio;
  - Flow observables, deformation

Thank you for your attention!

Haojie Xu(徐浩洁)

Huzhou University(湖州师范学院)

Backup

Uncertainties from nuclear deformation

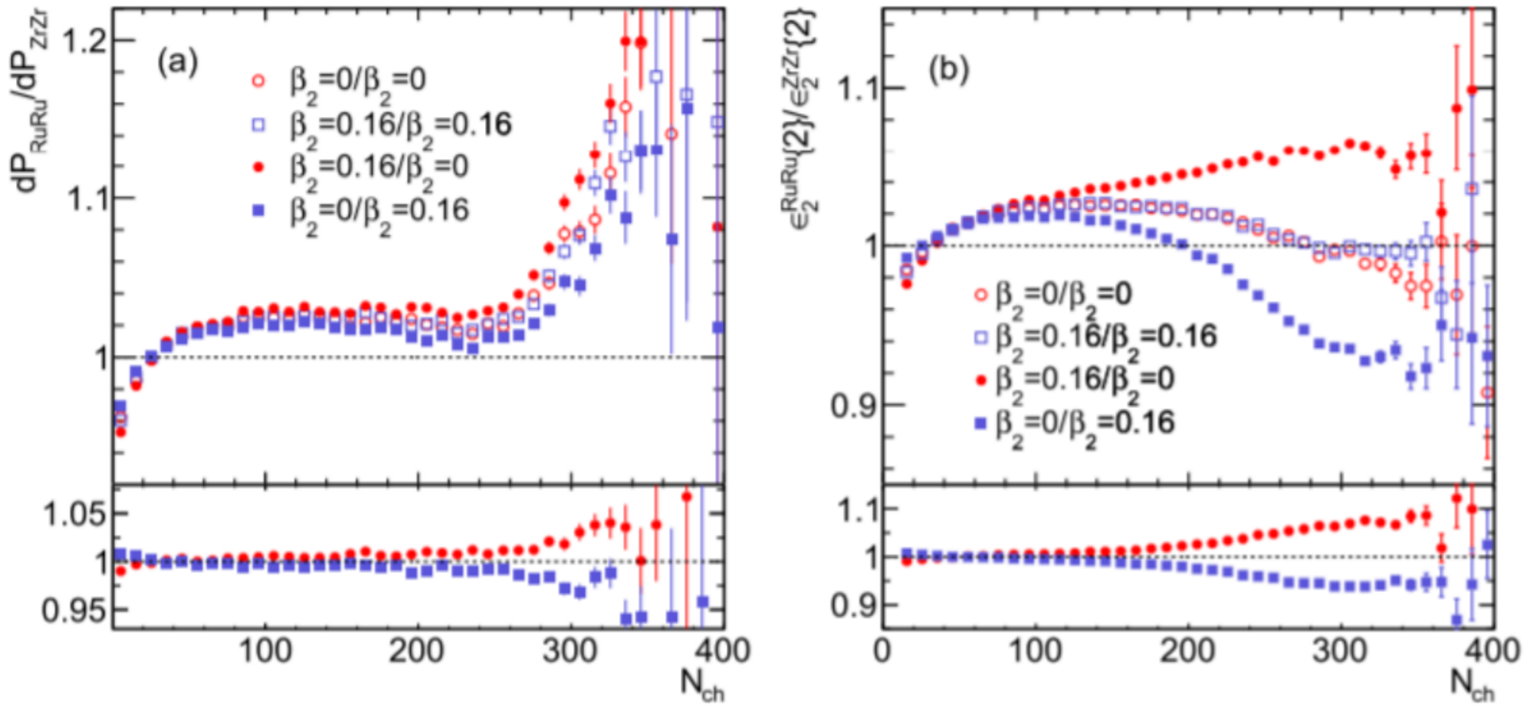

HJX, et.al., PLB819, 136453 (2021)

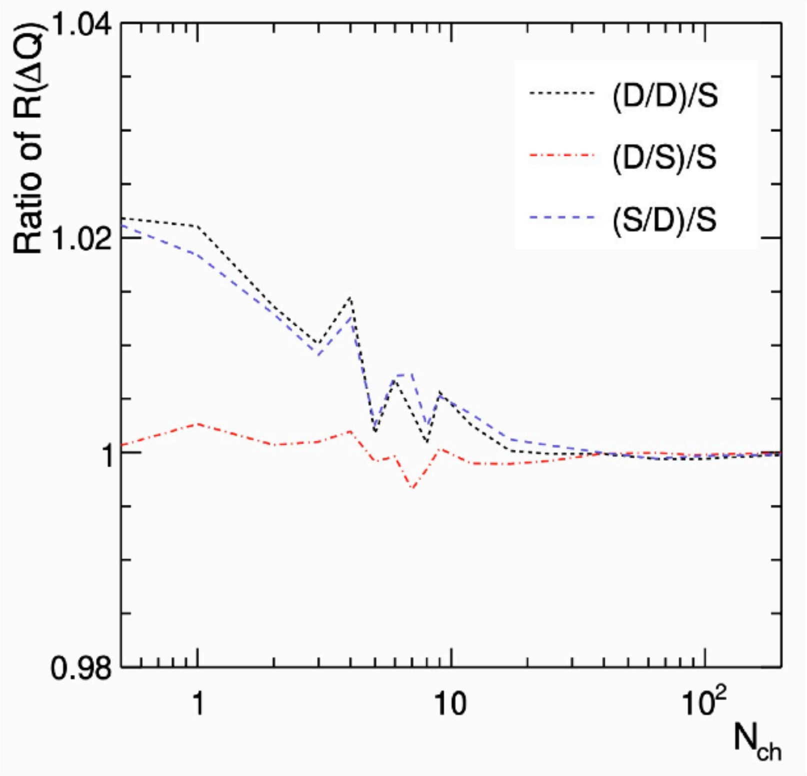

HJX, et.al., arXiv:2105.04052 (2021)

Flow differences in isobar collisions:

- Nuclear size and nuclear shape should be simultaneously studied.
- The non-flow effect, fluctuation and correlations, hydrodynamic response need to be considered for the flow study.

Background differences

STAR Collaboration, arXiv:2109.00131

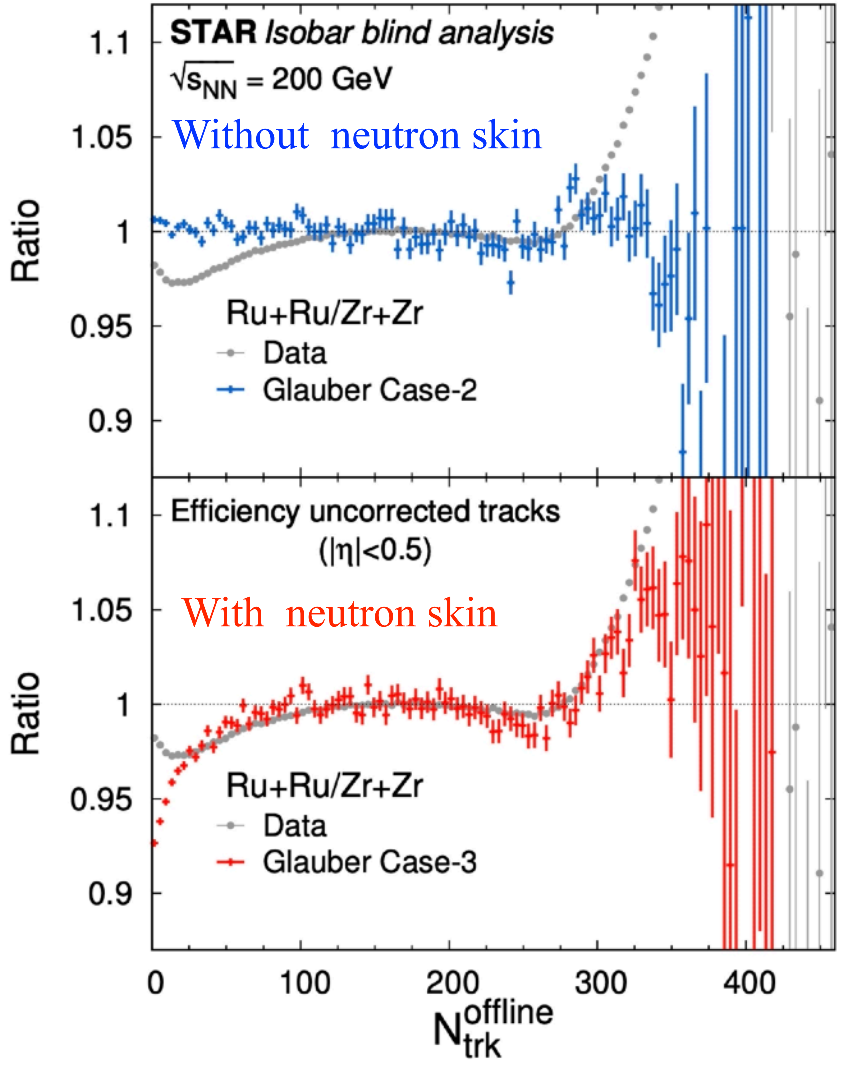

multiplicity distributions are different

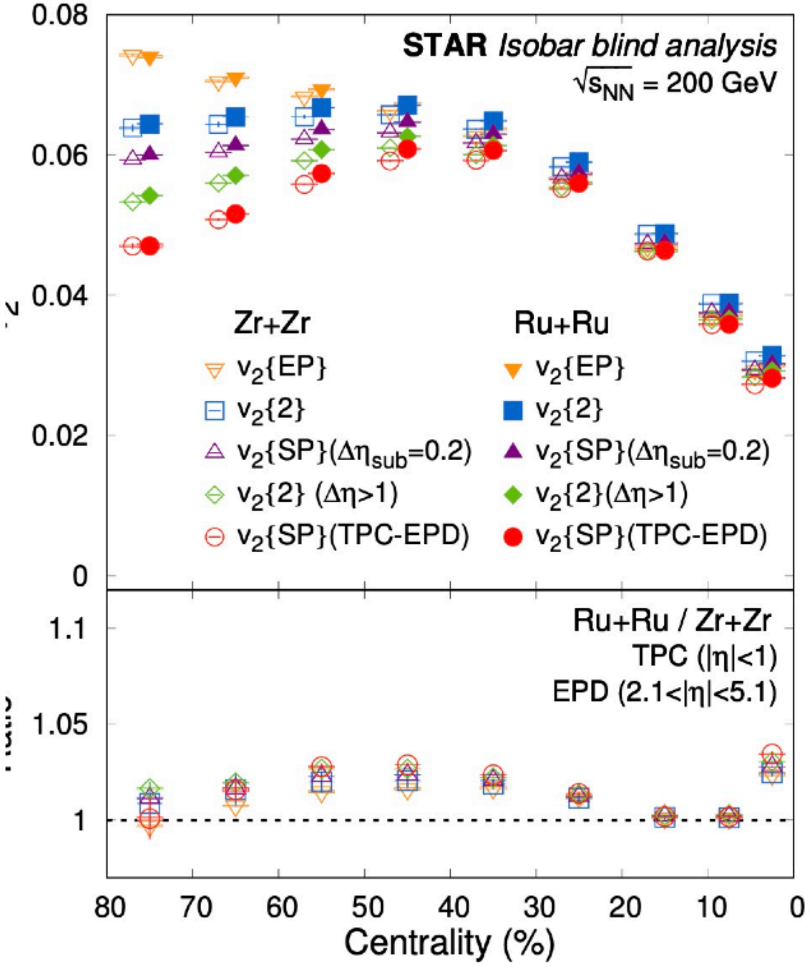

v_2 are different

- Obvious differences **in v_2 and** $P(N_{ch})$ at 20-50% centrality, as well as large enhancement of $P(N_{ch})$ **ratios at most central collisions**, as predicted by the calculation with DFT densities, but contrary to the predictions with charge density distributions.
- Sizable v_2 and v_3 ratios at most central collisions may indicate shape difference in isobars. (Jiangyong's talk)

Determine the neutron skin type in isobar collisions

HJX, et.al., PLB819, 136453 (2021)

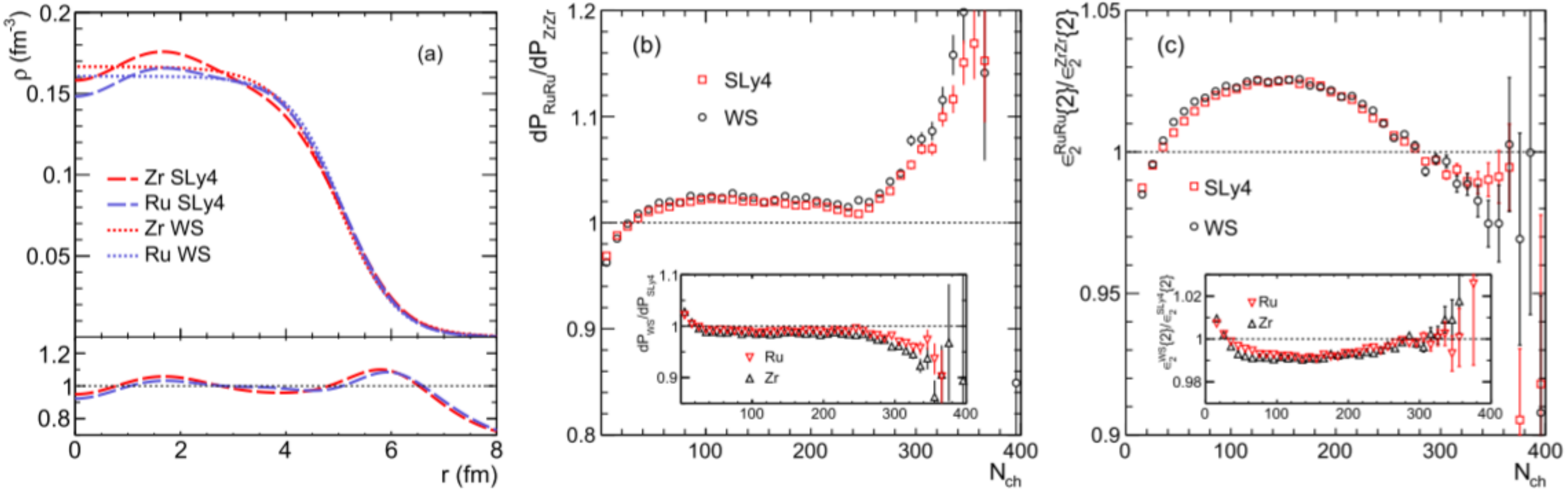

The halo-type density can serve as a good surrogate for the DFT density.

- DFT and WS
  - $\langle r \rangle_{DFT} = \langle r \rangle_{WS}$
  - $\sqrt{\langle r^2 \rangle_{DFT}} = \sqrt{\langle r^2 \rangle_{WS}}$

	^{96}Ru		^{96}Zr	
	R	*a*	*R*	*a*
p	5.060	0.493	4.915	0.521
n	5.075	0.505	5.015	0.574
p+n	5.067	0.500	4.965	0.556

Case 3